European Journal of Radiology 120 (2019) 108686

Contents lists available at ScienceDirect

European Journal of Radiology

journal homepage: www.elsevier.com/locate/ejrad

Research article

# Intravoxel incoherent motion diffusion-weighted MRI in patients with breast cancer: Correlation with tumor stroma characteristics

Li Yuan[a], Zhengping Wang[a], Feng Chen[a,*], Xin Qin[a], Changqing Li[a], Yingman Zhao[a], Chenggong Yan[b], Yuankui Wu[b], Peng Hao[b], Yikai Xu[b]

[a] Department of Radiology, Hainan General Hospital, Haikou, Hainan, 570311, China
[b] Department of Medical Imaging Center, Nanfang Hospital, Southern Medical University, Guangzhou, Guangdong, 510515, China

ARTICLE INFO

*Keywords:*
Breast cancer
Magnetic resonance imaging (MRI)
Intravoxel incoherent motion (IVIM)
Tumor stroma ratio (TSR)

ABSTRACT

*Purpose:* To determine whether imaging parameters derived from intravoxel incoherent motion (IVIM) diffusion weighted imaging (DWI) vary according to tumor-stroma ratio(TSR) or dominant stroma type of breast cancer.
*Methods:* We prospectively enrolled 77 patients with breast cancer who underwent IVIM DWI on a 3.0 T MR scanner. The values of IVIM parameters (D, D* and f) were measured. After surgery, TSR or dominant stroma type was evaluated. The relationship between imaging parameters and tumor stroma characteristics was analyzed.
*Results:* The mean D and f values were lower in stroma-poor tumor than in stroma-rich tumor ($P = 0.012$, 0.015). The mean D value was lower in the collagen-dominant type than in fibroblast-dominant or lymphocyte-dominant type ($P = 0.032$, 0.043). According to multivariate linear regression analyses, tumor size ($P = 0.007$), TSR ($P = 0.008$), dominant stroma type (collagen dominant, $P = 0.012$), and histological grade ($P = 0.031$) were independently correlated with D value; and tumor size ($P = 0.011$), TSR ($P = 0.021$) and histological grade ($P = 0.037$) were independently correlated with f value.
*Conclusion:* In breast cancer, D and f values show significant differences according to TSR, and D value is lower in collagen dominant type than in fibroblast dominant or lymphocyte dominant types.

## 1. Introduction

The tumor stroma plays an active role in supporting and nourishing tumor cells and is closely related to tumor malignant behavior, such as progression, invasion and metastasis [1]. The previous studies [2–4] suggested that TSR and dominant stroma type were independent prognostic factors in pulmonary, oral and mammary cancer. The study by Wu et al [5] showed that higher TSR were related to worse survival in patients with solid tumor. According to the study by Ahn et al [6], the breast tumor with collagen predominant type frequently had a poor prognosis. Therefore, the quantitative assessment of TSR or dominant stroma type is very useful for elucidating the disease mechanism or predicting the prognosis of breast cancer.

DWI has been considered to be a convenient technique for assessing tumor stroma characteristics of breast tumors [7,8]. Ko et al [9] found that there was a significant difference in ADC values among different TSRs or dominant stroma types of breast cancers. However, both pure molecular diffusion and microcirculation perfusion contribute to ADC value, which may impair the ability of ADC in characterizing tumor micro-structure [10], while IVIM technique can separate perfusion from diffusion on the basis of a bi-exponential model analysis by using multiple b-values. IVIM DWI can reflect the tumor micro-structure more accurately [11]. Li et al [12] explored the correlation between IVIM parameters and TSR of cervical cancer, and found that D and f values were independently correlated with TSR. However, up to now, there has been no study on the exploration of the relationship between IVIM parameters and TSR or dominant stroma type of breast cancer.

Accordingly, the purpose of this study is to determine whether IVIM parameters vary according to TSRs or dominant stroma types, and to investigate the relationship between IVIM parameters and tumor stroma characteristics of breast cancers.

## 2. Methods

### 2.1. Patient selection

This is a prospective observational clinical single-center study. This study was approved by the local ethics committee of our hospital

* Corresponding author at: Department of Radiology, Hainan General Hospital, No.19 Xiuhua Avenue, Haikou, Hainan Province, 570311, China.
*E-mail address:* chenfeng1122@aliyun.com (F. Chen).

https://doi.org/10.1016/j.ejrad.2019.108686
Received 21 July 2019; Received in revised form 15 September 2019; Accepted 18 September 2019

(Approval No. 2014-0123), and all the patients were informed and gave their written consent to participate in this study. Between August 21, 2013 and December 30, 2018, 100 patients were invited to enroll in this study because of primary breast cancer. The inclusion criteria were as follows: (a) The patients were suspected to have breast cancer and the diagnosis was pathologically confirmed; (b) The lesion appeared as mass on MRI, the largest diameter of tumor was 1 ~ 4 cm and there was no axillary lymph node metastasis or distant metastasis; (c) The patients didn't undergo neoadjuvant chemotherapy; (d) The time interval between MR examination and surgery was ≤ 5 days. The exclusion criteria included: (a) There was a contraindication to MRI examination (such as allergy to contrast media or claustrophobia); (b) There was imaging failure (such as severe artifact or failure of fat suppression); (c) The pathologic data were not complete. Finally, 77 patients were included into this study.

### 2.2. MRI technique

MRI examinations were performed on a whole-body 3.0 T MR scanner (Discovery MR750, GE Healthcare, USA) with an 8-channel phased-array breast coil. All the patients were imaged in the prone position. First, the conventional MRI sequences were performed. Then, IVIM DWI sequence was performed. Finally, dynamic contrast-enhanced (DCE) MRI was performed.

The conventional MRI sequences included axial fat suppression T1WI (TR/TE: 170/2.8 ms) and T2WI (TR/TE: 3500/70 ms). The main parameters were as follows: slice thickness: 5.0 mm; inter-slice gap: 0.5 mm; field of vision (FOV): 34 cm × 34 cm; matrix size: 269 × 384.

IVIM DWI sequence was acquired by using an STIR fat-saturated, single-shot, spin-echo echo-planar imaging (SE-EPI). Twelve b values of 0, 10, 20, 30, 50, 70, 100, 150, 200, 400, 800 and 1000s/mm$^2$ were selected. The number of excitation (NEX) was 1, 3, 3, 3, 3, 2, 2, 2, 3, 3, 5 and 6 respectively. The other main parameters were as follows: TR/TE: 3000/93.6 ms; FOV: 34 cm × 34 cm; matrix size:128 × 160; slice thickness: 5 mm; inter-slice gap: 1 mm; receiver bandwidth: 250 kHz; and parallel imaging (ASSET) factor: 2. The imaging duration was 8 min and 21 s.

The axial multi-phase 3D Vibrant-Flex DCE MRI was acquired before and repeated 8 times(duration 45 s each) after intravenous injection of 0.2 mmol/kg Gd-DTPA (Magnevist; Bayer, Germany), followed by 20 mL saline flush. The contrast media was injected at antecubital vein via a power injector. The main parameters were as follows: TR/TE: 4.48/1.65 ms; FOV: 34 cm × 34 cm; matrix size: 352 × 260; slice thickness: 1 mm; inter-slice gap: 0.25 mm; flip angle: 10°.

### 2.3. Analysis of MR images

The original imaging data were transferred to GE AW 4.6 workstation for further analysis. The images were independently processed and analyzed by two radiologists who had 10 and 8 years of experience in breast MRI respectively. If the lesion appeared as multifocal, only the index lesion was selected for imaging analysis. They were blinded to all the clinicopathologic data except that the patients suffered from breast cancer. Region of interest (ROI) was manually placed on DW images with a b value of 800 s/mm$^2$ at the slice of maximum transverse diameter of tumor under the guidance of DCE MR images. ROI should cover as much of tumor area as possible, and should avoid the recognizable necrotic, hemorrhagic and cystic areas. In addition, ROI should contain at least 5 pixels when the tumor was small.

In IVIM model, the relationship between signal intensity and b factors was determined according to the following equation [13]:

$$Sb = (1\text{-}f) \times \exp(-b \cdot D) + f \times \exp[-b(D^* + D)]$$

D* was the pseudo-diffusion coefficient related to perfusion-related diffusion, D was the true diffusion coefficient that reflected the pure molecular diffusion, and f was the perfusion fraction representing the volume fraction of microcirculation. The IVIM parameters were calculated on the basis of the assumption that D* was significantly larger than D, and the effects of D* on the signal decay at high b-values (> 200 s/mm$^2$) could be neglected [14].

**Table 1**
Comparisons of clinicopathologic factors according to TSR.

| Parameters | TSR | | *P*-value |
|---|---|---|---|
| | Stroma-rich(n = 31) | Stroma-poor(n = 46) | |
| Mean tumor size(mm)* | 14.4 ± 4.1 | 19.8 ± 6.9 | 0.031 |
| Age(y)* | 43.0 ± 9.0 | 41.0 ± 6.0 | 0.379 |
| Pathological type(n) | | | 0.121 |
| IDC | 24(77.4) | 37(80.4) | |
| Other types | 7(22.6) | 9(19.6) | |
| Dominant stroma type(n) | | | 0.105 |
| Fibroblast | 23(74.2) | 25(54.3) | |
| Collagen | 5(16.1) | 13(28.3) | |
| Lymphocyte | 3(9.7) | 8(17.4) | |
| Histological grade(n) | | | 0.023 |
| I | 20(64.5) | 12(26.1) | |
| II | 8(25.8) | 15(32.6) | |
| III | 3(9.7) | 19(41.3) | |
| Genomic subtype(n) | | | 0.167 |
| Luminal A | 16(51.6) | 22(47.8) | |
| Luminal B | 7(22.6) | 10(21.7) | |
| Basal like | 4(12.9) | 5(10.9) | |
| Her2-enriched | 4(12.9) | 9(19.6) | |

*Note.*-TSR: tumor stroma ratio; IDC: invasive ductal carcinoma.
* Data are expressed as mean size ± standard deviation; The numbers in parenthesis are percentages.

### 2.4. Histopathological analysis

Under the guidance of MRI images, surgical specimens of the macroscopic tumor were serially sliced at 5 mm thickness, and stained with hematoxylin–eosin (HE). The section of maximum transverse diameter of tumor area was selected and used for pathological analysis. According to the method used by Ko et al [9], TSR was estimated visually and scored per tenfold percentage as follows: stroma-rich group (< 50% tumor percentage) and stroma-poor group (≥50% tumor percentage). Three stromal components, including collagen, fibroblasts and lymphocytes, were determined on the basis of its dominant stroma type [6].

The histological grades were evaluated according to tubule formation, pleomorphism and mitotic counts, and scored as follows: grade I (well differentiated), grade II (moderately differentiated) and grade III (poorly differentiated) [15].

### 2.5. Statistical analysis

All the statistical analyses were performed with SPSS version 20.0 (Chicago, IL, USA). Interobserver agreement was analyzed for the mean value of imaging parameters by calculating the concordance correlation coefficient (CCC). The evaluation criteria for CCC were as follows: > 0.95, good agreement; 0.90-0.95, moderate agreement; and < 0.90, poor agreement [16].

The differences in clinical or histopathological characteristics between stroma-rich and stroma-poor tumor were determined by using Mann-Whitney *U* test or Fisher's exact test. The comparisons of imaging parameters between stroma-rich and stroma-poor tumor were performed by using Mann-Whitney *U* test. The differences in imaging parameters among different dominant stroma types were determined by using Kruskal-Wallis test, and post hoc comparisons were furtherly conducted for continuous measurements if the test result was statistically significant. Multivariate linear regression analysis was carried out to determine variables independently associated with D or f value.

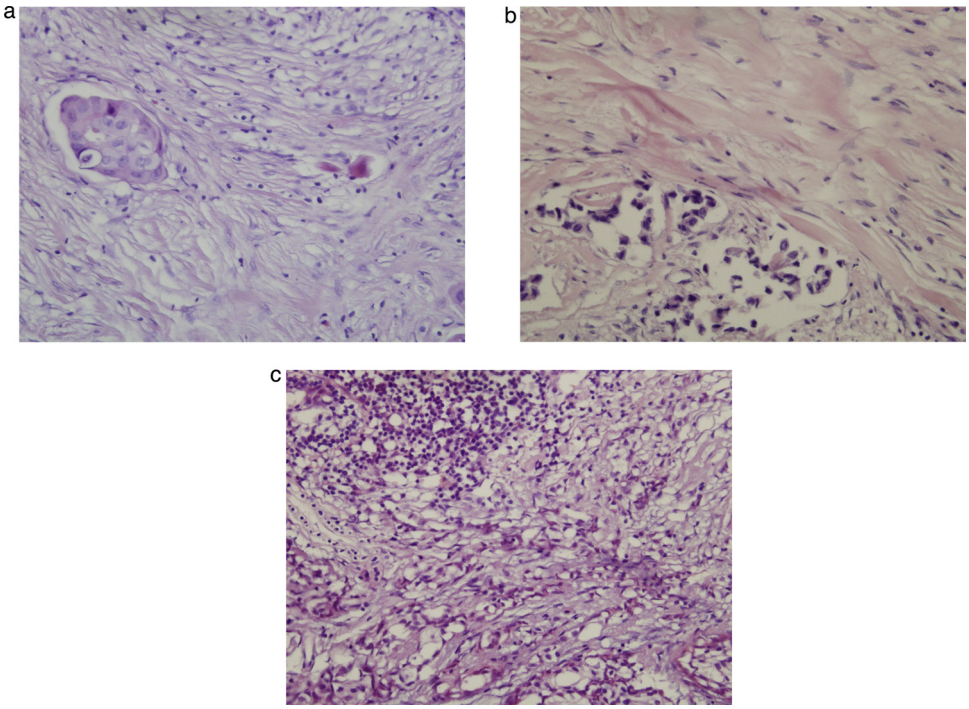


**Fig. 1.** The dominant stroma cell types of breast cancers (×400).
(a) The tumor stroma appeared as fibroblast-dominant type.
(b) The tumor stroma appeared as collagen-dominant type.
(c) The tumor stroma appeared as lymphocyte dominant type.

**Table 2**
Interobserver agreement of IVIM parameters.

| Parameters | Observer 1 | Observer 2 | CCC(95%CI) |
|---|---|---|---|
| D($10^{-3}$/mm$^2$) | 0.63 ± 0.23 | 0.62 ± 0.21 | 0.94 (0.85～0.96) |
| D*($10^{-3}$/mm$^2$) | 11.12 ± 1.45 | 11.09 ± 1.41 | 0.90 (0.80～0.93) |
| f (%) | 28.69 ± 4.76 | 28.75 ± 4.85 | 0.91 (0.82～0.93) |

*Note.* −CCC: concordance correlation coefficient; CI: confidence interval.

Statistical significance was set at a level of $P < 0.05$.

## 3. Results

### 3.1. The comparisons of clinicopathologic factors according to TSR

The clinical and histopathological findings were seen in Table 1. According to statistical analysis, stroma-poor tumor was larger than stoma-rich tumor ($P = 0.031$). In stroma-poor tumor, there was higher percentage of the tumor with high histological grade ($P = 0.023$). The dominant stroma type was classified into fibroblast dominant (n = 48), collagen dominant (n = 18) and lymphocyte dominant(n = 11) (Fig. 1). There was no significant difference in dominant stroma type between stoma-rich and stroma-poor tumor ($P = 0.105$).

### 3.2. The value of IVIM parameters according to tumor stroma characteristics

There was a moderate interobserver agreement on the measurement of D, D* or f value (CCC = 0.94, 0.90, 0.91) (Table 2).

The values of imaging parameters according to tumor stroma characteristics were seen in Table 3. D and f values were significantly lower in stroma-poor tumor than in stroma-rich tumor ($P = 0.012$, 0.015) (Figs. 2 and 3), and there was no significant difference in D* value between two groups ($P = 0.071$). D value was lower in collagen dominant type than in fibroblast dominant or lymphocyte dominant type ($P = 0.032$, 0.043). D and f values were higher in well/moderately

**Table 3**
The values of imaging parameters according to histological characteristics.

| Items | D($10^{-3}$/mm$^2$) | *P*-value | D*($10^{-3}$/mm$^2$) | *P*-value | f (%) | *P*-value |
|---|---|---|---|---|---|---|
| TSR | | 0.012 | | 0.071 | | 0.015 |
| Stroma-rich | 0.70 ± 0.38 | | 12.01 ± 6.63 | | 37.05 ± 11.34 | |
| Stroma-poor | 0.52 ± 0.24 | | 10.23 ± 5.09 | | 20.32 ± 6.34 | |
| Dominant stroma type | | 0.011* | | 0.124 | | 0.071 |
| Collagenous | 0.40 ± 0.15 | | 10.01 ± 5.24 | | 20.23 ± 8.34 | |
| Fibroblastic | 0.57 ± 0.32 | | 9.11 ± 4.23 | | 35.23 ± 10.21 | |
| Lymphocytic | 0.71 ± 0.29 | | 12.21 ± 6.23 | | 25.67 ± 6.23 | |
| Histological grade | | 0.022 | | 0.106 | | 0.026 |
| well/moderately differentiated | 0.73 ± 0.31 | | 11.23 ± 4.23 | | 31.23 ± 10.23 | |
| Poorly differentiated | 0.45 ± 0.25 | | 9.79 ± 5.34 | | 23.62 ± 9.04 | |

*Note.*-TSR: tumor stroma ratio; Data are expressed as mean size ± standard deviation.
* The further analysis by using post hoc comparisons showed that the D value was lower in collagen dominant type than in fibroblast dominant or lymphocyte dominant type ($P = 0.032$, 0.043).

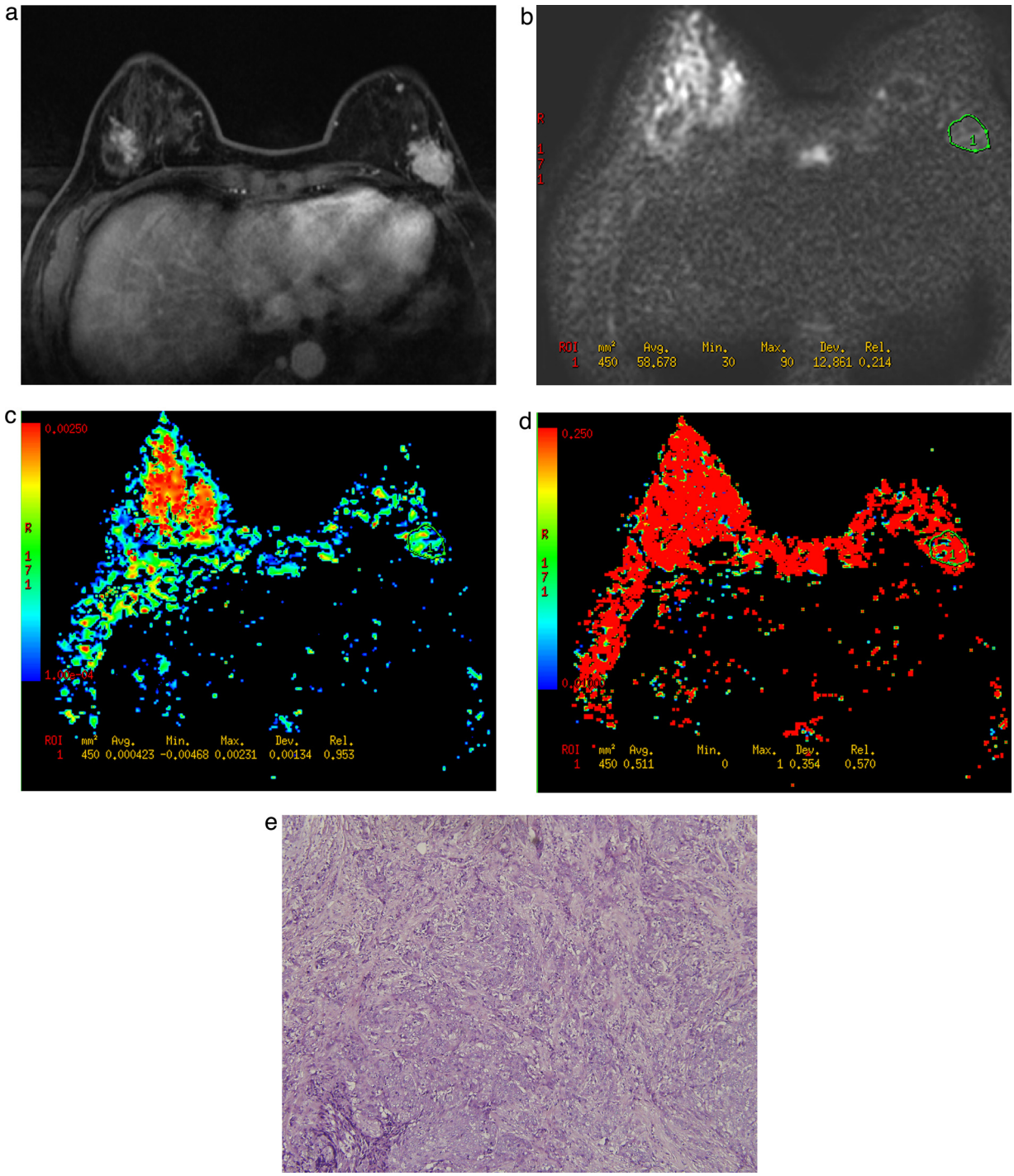


**Fig. 2.** The value of IVIM parameters in stroma-poor tumor. A 53-year-old woman with proven micropapillary breast cancer.
(a) Axial contrast-enhanced image, there was a mass in left breast.
(b) Axial DW image, the image showed the location of ROI within the tumor area.
(c) D map, D value was relatively low ( = 0.423 × 10−3 mm2/s).
(d) f map, f value was slightly low ( = 51.1%).
(e) H—E stained section of tumor (×200), TSR was classified as stroma-poor group (stroma percentage = 10%).

differentiated tumor than in poorly differentiated tumor ($P$ = 0.022, 0.026).

### 3.3. The relationship between IVIM parameters and tumor stroma characteristics

The results of the residual analysis satisfied the assumption of linearity, independence, normality and equal variance. According to multivariate line regression analysis, tumor size ($P$ = 0.007), TSR ($P$ = 0.008), dominant stroma type (collagen dominant, $P$ = 0.012) and histological grade ($P$ = 0.031) were independently correlated with D value (Table 4). Tumor size ($P$ = 0.011), TSR ($P$ = 0.021) and histological grade ($P$ = 0.037) were independently correlated with f value (Table 5).

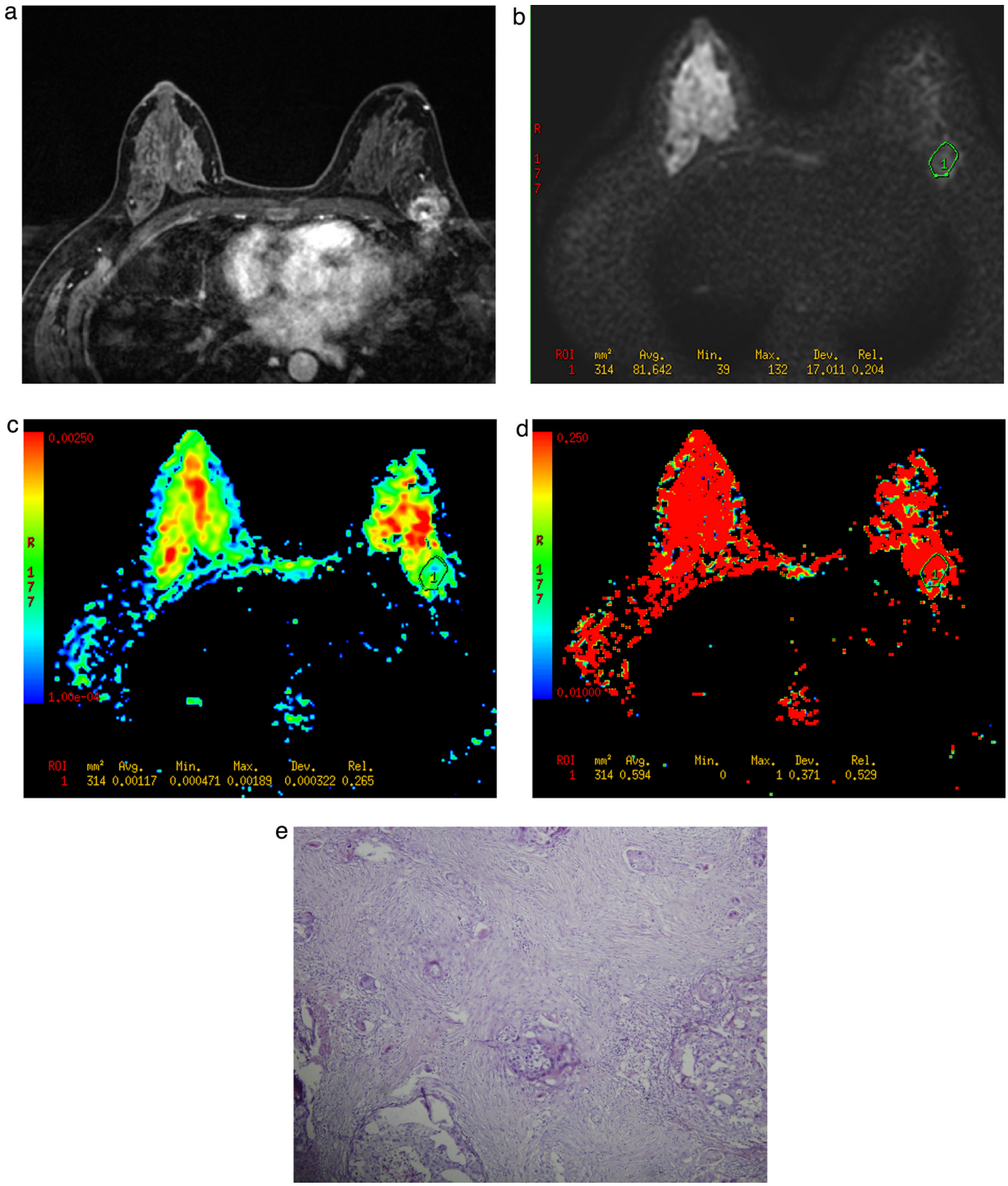


**Fig. 3.** The value of IVIM parameters in stroma-rich tumor. A 37-year-old woman with proven invasive ductal breast cancer.
(a) Axial contrast-enhanced image, there was a mass in left breast.
(b) Axial DW image, the image showed the location of ROI within the tumor area.
(c) D map, D value was relatively high ( = 1.17 × 10−3 mm2/s).
(d) f map, f value was slightly high ( = 59.4%).
(e) H—E stained section of tumor (×200), TSR was classified as stroma-rich group (stroma percentage = 80%).

## 4. Discussion

There have been a few studies [9,17,18] to explore the relationship between imaging parameters and tumor stroma characteristics of breast cancers. Ko et al [9] explored the relationship between ADC value and TSR of breast cancer, and found that ADC value was lower in collagen dominant type than in fibroblast or lymphocyte dominant type. Yim et al [17] evaluated TSR of breast cancer by using DCE MRI, and found that $V_e$ value was significantly lower in tumor with high TSR, and $K_{ep}$ value was significantly lower in tumor with dominant collagen type. Balleyguier et al [18] investigated the value of magnetic resonance elastography (MRE) combined with MRI in assessing tumor stroma characteristics, and suggested that this imaging technique was very useful for tumor stroma characterization. However, any imaging

**Table 4**
Multiple linear regression analysis of variables independently associated with D value.

| Parameter | β | β' | 95% CI for β level | *P*-value |
|---|---|---|---|---|
| Tumor size | −0.013 | −0.331 | −0.021, -0.010 | 0.007 |
| TSR | −0.021 | −0.319 | −0.033, -0.012 | 0.008 |
| Dominant stroma type | | | | |
| Fibroblast | −0.011 | 0.021 | −0.021,-0.008 | 0.789 |
| Collagen | −0.113 | 0.047 | −0.219, -0.011 | 0.012 |
| Lymphocyte | −0.032 | 0.073 | −0.206, 0.119 | 0.654 |
| Histological grade | −0.050 | 0.064 | −0.184, 0.175 | 0.031 |

TSR: tumor stroma ratio; 95% CI: 95% confidence interval.

**Table 5**
Multiple linear regression analysis of variables independently associated with f value.

| Parameter | β | β' | 95% CI for β level | *P*-value |
|---|---|---|---|---|
| Tumor size | −0.032 | −0.198 | −0.006, -0.001 | 0.011 |
| TSR | −0.013 | −0.319 | −0.022, 0.004 | 0.021 |
| Histological grade | −0.048 | 0.052 | −0.179, 0.118 | 0.037 |

TSR: tumor stroma ratio; 95% CI: 95% confidence interval.

parameter mentioned above is not adequate to serve as a sensitive and reliable marker for tumor stroma characteristics in clinical settings. It is necessary to introduce a more reliable imaging technique for evaluating TSR or dominant stroma type of breast cancer.

To our knowledge, this is the first study to explore the relationship between IVIM parameters and dominant stromal types of breast cancers. This study showed that D value was lower in collagen-dominant type than in fibroblast-dominant or lymphocyte-dominant type. The possible reason is that collagen-dominant stroma increases the tortuosity and heterogeneity of tumor micro-structure, interstitial fluid pressure and osmotic pressure, which inhibits the true water diffusion, and subsequently results in the decreased D value [9,19].

This study showed that D value was significantly lower in stroma-poor tumor than in stroma-rich tumor. Similarly, Li et al [12] investigated the correlation between D value and TSR of cervical cancer, and found that D value was lower in the tumor with higher TSR. The possible explanation for these results is that stroma-rich tumor has bigger extracellular and extravascular spaces, and thus pure water diffusion motion becomes more unrestricted, which results in the increased D value, whereas stroma-poor tumor has restricted intracellular and extracellular water diffusion, which results in the decreased D value [20].

The f value reflects the proportion of perfusion of microcirculation in tissue diffusion. Li et al [12] found that there was a moderately negative correlation between TSR and f value. This study also showed that f value was higher in stroma-rich tumor than in stroma-poor tumor. It is possible that the apparent link between f and stromal volume might be an artifact coming from residual diffusion effects in the stroma, but the further study is necessary in order to clarify the definite correlation between f value and TSR. Compared with previous studies [10,14], f values acquired by us were fairly higher. This may be driven by the inclusion criteria of large malignant, untreated masses (1–4 cm), and the explicit avoidance of necrotic/cystic areas in sampling.

D∗ value reflects the pseudodiffusion coefficient produced by microcirculation perfusion, and is mainly related to the length of capillaries in microcirculation perfusion and blood flow velocity [21]. This study showed that D∗ value was slightly higher in stroma-rich tumor than in stroma-poor tumor, but the difference didn't achieve a significance level. Theoretically, D* value has some technical limitations, such as great standard deviation, data instability and its dependence on signal noise ratio (SNR) [12,22], therefore, D* is very difficult to model and measure sensitively and accurately, which may be the main reason for no significant correlation between D* value and TSR.

We investigated the relationship between IVIM parameters and histological grades of breast cancers, and found that poorly differentiated tumor had lower D or f value than well/moderately differentiated tumor, while there was no significant difference in D* value between two groups. In contrast, the previous study by Ichikawa et al [23] investigated the correlations between IVIM parameters and histological grades of hepatocellular cancers, and found that there were significant differences in all three parameters (D, D* and f) between poorly differentiated and well/moderately differentiated tumor. The inconsistency between two studies may be due to the difference in pathological types of tumor, the fitting methods of parameters, the setting of multiple b values or instability of D* value [23–25].

### 4.1. Limitations

Firstly, only the patients with early breast cancers were included into this study. Therefore, the results acquired by us may not be suitable for advanced breast cancers. Secondly, although we tried our best to achieve a good match between pathologic section and the corresponding imaging section, the precise area in which IVIM parameters and tumor stroma characteristics measured might still be slightly different [26]. Thirdly, the setting of multiple b values made a slight influence on the measurement of IVIM parameters and thus might bring about subtle evaluating bias [27]. Finally, ROI analysis only on the basis of the slice of maximum transverse diameter of tumor does not completely characterize each tumor's heterogeneity or guarantee sampling of its most malignant portion [28]. Therefore, the results acquired from this study might not be adequate to represent the situation of the total tumor area.

### 4.2. Conclusion

This study shows that D and f values obtained from IVIM DWI can reflect the detailed tumor stroma characteristics of breast cancer, including TSR and dominant stroma type, which is very useful for the clinical applications, such as elucidating the disease mechanism, planning breast carcinoma treatment and predicting prognosis.

## Declaration of Competing Interest

The authors declare that they have no competing interests.

## References

[1] N. Kemi, M. Eskuri, A. Herva, J. Leppänen, H. Huhta, O. Helminen, J. Saarnio, T.J. Karttunen, J.H. Kauppila, Tumour-stroma ratio and prognosis in gastric adenocarcinoma, Br. J. Cancer 119 (4) (2018) 435–439.
[2] K.X. Xi, Y.S. Wen, C.M. Zhu, Qin R.Q. Yu XY, X.W. Zhang, Y.B. Lin, T.H. Rong, W.D. Wang, Y.Q. Chen, L.J. Zhang, Tumor-stroma ratio (TSR) in non-small cell lung cancer (NSCLC) patients after lung resection is a prognostic factor for survival, J. Thorac. Dis. 9 (10) (2017) 4017–4026.
[3] K.C. Niranjan, N.A. Sarathy, Prognostic impact of tumor-stroma ratio in oral squamous cell carcinoma- a pilot study, Ann. Diagn. Pathol. 35 (2018) 56–61.
[4] C.L. Downey, S.A. Simpkins, J. White, D.L. Holliday, J.L. Jones, L.B. Jordan, J. Kulka, S. Pollock, S.S. Rajan, H.H. Thygesen, A.M. Hanby, V. Speirs, The prognostic significance of tumour-stroma ratio in oestrogen receptor-positive breast cancer, Br. J. Cancer 110 (7) (2014) 1744–1777.
[5] J. Wu, C. Liang, M. Chen, W. Su, Association between tumor-stroma ratio and prognosis in solid tumor patients: a systematic review and meta-analysis, Oncotarget. 7 (42) (2016) 68954–68965.
[6] S. Ahn, J. Cho, J. Sung, J.E. Lee, S.J. Nam, K.M. Kim, E.Y. Cho, The prognostic significance of tumor associated stroma in invasive breast carcinoma, Tumour Biol. 33 (5) (2012) 1573–1580.
[7] K. Yamaguchi, Y. Hara, I. Kitano, T. Hamamoto, K. Kiyomatsu, F. Yamasaki, R. Egashira, R. Egashira, T. Nakazono, H. Irie, Tumor-stromal ratio (TSR) of invasive breast cancer: correlation with multi-parametric breast MRI findings, Br. J. Radiol. 92 (1097) (2019) 20181032.
[8] H.J. Shin, J.Y. Park, K.C. Shin, H.H. Kim, J.H. Cha, E.Y. Chae, W.J. Choi, Characterization of tumor and adjacent peritumoral stroma in patients with breast cancer using high-resolution diffusion-weighted imaging: correlation with pathologic biomarkers, Eur. J. Radiol. 85 (5) (2016) 1004–1011.

[9] E.S. Ko, B.K. Han, R.B. Kim, E.Y. Cho, S. Ahn, S.J. Nam, E.Y. Ko, J.H. Shin, S.Y. Hahn, Apparent diffusion coefficient in estrogen receptor-positive invasive ductal breast carcinoma: correlations with tumor-stroma ratio, Radiology 271 (1) (2014) 30–37.
[10] X. Mao, X. Zou, N. Yu, X. Jiang, J. Du, Quantitative evaluation of intravoxel incoherent motion diffusion-weighted imaging (IVIM) for differential diagnosis and grading prediction of benign and malignant breast lesions, Medicine (Baltimore) 97 (26) (2018) e11109.
[11] S.C. Zhu, Y.H. Liu, Y. Wei, L.L. Li, S.W. Dou, T.Y. Sun, D.P. Shi, Intravoxel incoherent motion diffusion-weighted magnetic resonance imaging for predicting histological grade of hepatocellular carcinoma: comparison with conventional diffusion-weighted imaging, World J. Gastroenterol. 24 (8) (2018) 929–940.
[12] X. Li, P. Wang, D. Li, H. Zhu, L. Meng, Y. Song, L. Xie, J. Zhu, T. Yu, Intravoxel incoherent motion MR imaging of early cervical carcinoma: correlation between imaging parameters and tumor-stroma ratio, Eur. Radiol. 28 (5) (2018) 1875–1883.
[13] Y. Zhu, X. Li, F. Wang, J. Zhang, W. Li, Y. Ma, J. Qi, S. Ren, Z. Ye, Intravoxel incoherent motion diffusion-weighted magnetic resonance imaging in characterization of axillary lymph nodes: preliminary animal experience, Magn. Reson. Imaging 52 (2018) 46–52.
[14] E.E. Sigmund, G.Y. Cho, S. Kim, M. Finn, M. Moccaldi, J.H. Jensen, D.K. Sodickson, J.D. Goldberg, S. Formenti, L. Moy, Intravoxel incoherent motion (IVIM) imaging of tumor microenvironment in locally advanced breast cancer, Magn. Reson. Med. 65 (5) (2011) 1437–1447.
[15] S. Zhao, W. Guo, R. Tan, P. Chen, Z. Li, F. Sun, G. Shao, Correlation between minimum apparent diffusion coefficient values and the histological grade of breast invasive ductal carcinoma, Oncol. Lett. 15 (5) (2018) 8134–8140.
[16] A.S. Littooij, P.D. Humphries, ØE Olsen, Intra- and interobserver variability of whole-tumour apparent diffusion coefficient measurements in nephroblastoma: a pilot study, Pediatr. Radiol. 45 (11) (2015) 1651–1660.
[17] H. Yim, D.K. Kang, Y.S. Jung, G.S. Jeon, T.H. Kim, Analysis of kinetic curve and model-based perfusion parameters on dynamic contrast enhanced MRI in breast cancer patients: correlations with dominant stroma type, Magn. Reson. Imaging 34 (1) (2016) 60–65.
[18] C. Balleyguier, A.B. Lakhdar, A. Dunant, M.C. Mathieu, S. Delaloge, R. Sinkus, Value of whole breast magnetic resonance elastography added to MRI for lesion characterization, NMR Biomed. 31 (1) (2018), https://doi.org/10.1002/nbm.3795.
[19] M. Iima, M. Kataoka, S. Kanao, N. Onishi, M. Kawai, A. Ohashi, R. Sakaguchi, M. Toi, K. Togashi, Intravoxel incoherent motion and quantitative non-Gaussian diffusion MR imaging: evaluation of the diagnostic and prognostic value of several markers of malignant and benign breast lesions, Radiology 287 (2) (2018) 432–441.
[20] Y. Kim, K. Ko, D. Kim, C. Min, S.G. Kim, J. Joo, B. Park, Intravoxel incoherent motion diffusion-weighted MR imaging of breast cancer: association with histopathological features and subtypes, Br. J. Radiol. 89 (1063) (2016) 20160140.
[21] E.Y. Lee, X. Yu, Q. Chu MM Chan, P.L. Khong, Perfusion and diffusion characteristics of cervical cancer based on intraxovel incoherent motion MR imaging-a pilot study, Eur. Radiol. 24 (7) (2014) 1506–1513.
[22] S. Ichikawa, U. Motosugi, D. Hernando, H. Morisaka, N. Enomoto, M. Matsuda, H. Onishi, Histological grading of hepatocellular carcinomas with intravoxel incoherent motion diffusion-weighted imaging: inconsistent results depending on the fitting method, Magn. Reson. Med. Sci. 17 (2) (2018) 168–173.
[23] A. Surov, H.J. Meyer, A.K. Höhn, C. Behrmann, A. Wienke, R.P. Spielmann, N. Garnov, Correlations between intravoxel incoherent motion (IVIM) parameters and histological findings in rectal cancer: preliminary results, Oncotarget. 8 (13) (2017) 21974–21983.
[24] S.C. Partridge, C.D. Mullins, B.F. Kurland, M.D. Allain, W.B. DeMartini, P.R. Eby, C.D. Lehman, Apparent diffusion coefficient values for discriminating benign and malignant breast MRI lesions: effects of lesion type and size, AJR Am. J. Roentgenol. 194 (6) (2010) 1664–1673.
[25] Y.C. Huang, T.W. Chen, X.M. Zhang, N.L. Zeng, R. Li, F. Chen, Y.L. Chen, Intravoxel incoherent motion diffusion-weighted imaging of resectable oesophageal squamous cell carcinoma: association with tumour stage, Br. J. Radiol. 91 (1084) (2018) 20170421.
[26] L. Zhu, L. Zhu, H. Shi, W. Chen, J. He, Z. Zhou, X. Yang, T. Liu, Evaluating early response of cervical cancer under concurrent chemo-radiotherapy by intravoxel incoherent motion MR imaging, BMC Cancer 16 (2016) 79–87.
[27] M. Iima, T. Nobashi, H. Imai, S. Koyasu, T. Saga, Y. Nakamoto, M. Kataoka, A. Yamamoto, T. Matsuda, K. Togashi, Effects of diffusion time on non-Gaussian diffusion and intravoxel incoherent motion (IVIM) MRI parameters in breast cancer and hepatocellular carcinoma xenograft models, Acta Radiol. Open 7 (1) (2018) 2058460117751565.
[28] A.S. Becker, J.A. Perucho, M.C. Wurnig, A. Boss, S. Ghafoor, P.L. Khong, E.Y.P. Lee, Assessment of cervical cancer with a parameter-free intravoxel incoherent motion imaging algorithm, Korean J. Radiol. 18 (3) (2017) 510–518.